

# Unraveling the history behind the FZ CMa's young stellar group

J. V. Corrêa-Rodrigues<sup>1</sup>, J. Gregorio-Hetem<sup>1</sup>, T. Santos-Silva<sup>1</sup>, & F. Almeida-Fernandes<sup>2</sup>

<sup>1</sup> Instituto de Astronomia, Geofísica e Ciências Atmosféricas da Universidade de São Paulo - IAG/USP  
e-mail: joaov.crodrigues@usp.br, gregorio-hetem@usp.br

<sup>2</sup> Observatório do Valongo - OV

**Abstract.** Investigating different star-forming regions is essential for understanding the formation and evolution of planets, stars, and also the Galaxy itself. This work aims to study the Canis Major OB1/R1 Association (CMa), which is a stellar nursery influenced by past supernovae. The primary goal is to improve the census of young stars in the region. Multi-object spectroscopy from the Gemini telescope was analysed to identify pre-main-sequence stars (PMS), particularly T Tauri stars (TT), in the direction of FZ CMa. Multiband photometric data from the Southern Photometric Local Universe Survey (S-PLUS) were used to characterize cloud members on a larger scale. Spectroscopic data revealed 29 TT stars and 7 PMS candidates by identifying typical spectral features such as H $\alpha$  emission and Li I ( $\lambda$  6708 Å) absorption. Accretion activity was examined based on the presence of H $\alpha$  and UV excess detected in S-PLUS data. The mean age of the S-PLUS sample was estimated at 5 Myr, which is consistent with values reported by other authors.

**Resumo.** Investigar diferentes regiões de formação estelar é essencial para entender a formação e evolução de planetas, estrelas e da própria Galáxia. Este trabalho busca estudar a Associação Canis Major OB1/R1 (CMa), que é um berçário estelar que foi influenciado por eventos de supernovas. O principal objetivo é melhorar o censo de estrelas jovens na região. Dados de espectroscopia multi-objeto do telescópio Gemini foram analisados para identificar estrelas da pré-sequência principal (PSP), particularmente estrelas T Tauri (TT), na direção de FZ CMa. Fotometria multibanda do *Southern Photometric Local Universe Survey* (S-PLUS) foi usada para caracterizar o membros da nuvem em maior escala. Os dados espectroscópicos revelaram a presença de 29 estrelas TT e 7 candidatas a estrelas PSP pela identificação de características espectrais típicas, como a emissão H $\alpha$  e a absorção do Li I ( $\lambda$  6708 Å). Atividade de acreção foi estudada com base na presença de excessos H $\alpha$  e UV, detectados com os dados S-PLUS. A idade média da amostra S-PLUS foi estimada em 5 Myr, que é um valor compatível com o reportado por outros autores.

**Keywords.** Stars: formation – Stars: pre-main sequence – Stars: variables: T Tauri, Herbig Ae/Be

## 1. Introduction

Pre-Main Sequence low-mass stars ( $0.5 M_{\odot} - 2 M_{\odot}$ ) are referred to as T Tauri stars (TTs). They are divided into two main classes: Classical T Tauri stars (CTTs) and Weak-lined T Tauri stars (WTTs). Both CTTs and WTTs have similar ages, with their youth indicated by the Li I ( $\lambda$  6708 Å) absorption line. These stars are also strong X-ray emitters (e.g. Feigelson & Montmerle 1999). On the other hand, while CTTs exhibit broad emission lines associated with accretion activity (specially H $\alpha$ ), WTTs have H $\alpha$  emission due to chromospheric activity. Consequently, WTTs have smaller H $\alpha$  equivalent widths ( $W_{H\alpha}$ ) compared with CTTs (Barrado y Navascués & Martín 2003).

The present work builds on the study presented in Corrêa-Rodrigues & Gregorio-Hetem (2024), and our main goal is to investigate the low-mass and young stellar population of CMa. Although previous studies have identified hundreds of young stars in CMa (e.g. Fernandes et al. 2015; Gregorio-Hetem et al. 2009, 2021), the *census* remains incomplete.

CMa is one of the most intriguing star-forming scenarios in the Milky Way. Evidence suggests that at least three supernova events from 6 to 1 Myr ago shaped CMa as part of a large shell-like structure ( $\sim 60$  pc of diameter — see Fernandes et al. 2019). These events may have affected the formation and evolution of members of CMa. One potential consequence is the early disruption of circumstellar disks, as noted by Fernandes et al. (2015).

Different star-forming regions may provide valuable insights into the processes governing the formation and evolution of the Galaxy. Moreover, star formation processes are intrinsically

linked to planetary system formation. In this sense, understanding the evolutionary history of CMa's stellar groups is crucial.

This paper is presented as follows. Section 2, outlines the methodology adopted to identify T Tauri stars and other PMS candidates based on multi-object spectroscopy. Section 3 describes an analysis of multiband photometric data from S-PLUS. Finally, a general summary and future perspectives are presented in Sect. 4.

## 2. GMOS spectroscopy

As described in Corrêa-Rodrigues & Gregorio-Hetem (2024), our group acquired spectroscopic data using the Gemini Multi-Object Spectrograph (GMOS), mounted on Gemini South telescope. 137 stars were observed across four fields, each with  $5.5' \times 5.5'$  Field of View (FoV). By adopting a maximum separation of  $10''$  between our targets and X-ray sources catalogued by Santos-Silva et al. (2018), we found that 17 % of our sample are X-ray emitters.

These objects are located in the "intercluster" region associated with FZ CMa (C field in Fig. 1). The stellar population in the west field, associated with GU CMa has a mean age exceeding 10 Myr. In contrast, the stellar population in the eastern field, associated with Z CMa, is younger, with a mean age of less than 5 Myr (Santos-Silva et al. 2018). These findings indicate that the population in the intercluster region has likely a mixture of ages.

To classify the stars in our sample as T Tauri stars or other PMS candidates, we searched for two main spectroscopic features of this evolutionary phase, as mentioned before: H $\alpha$  emis-

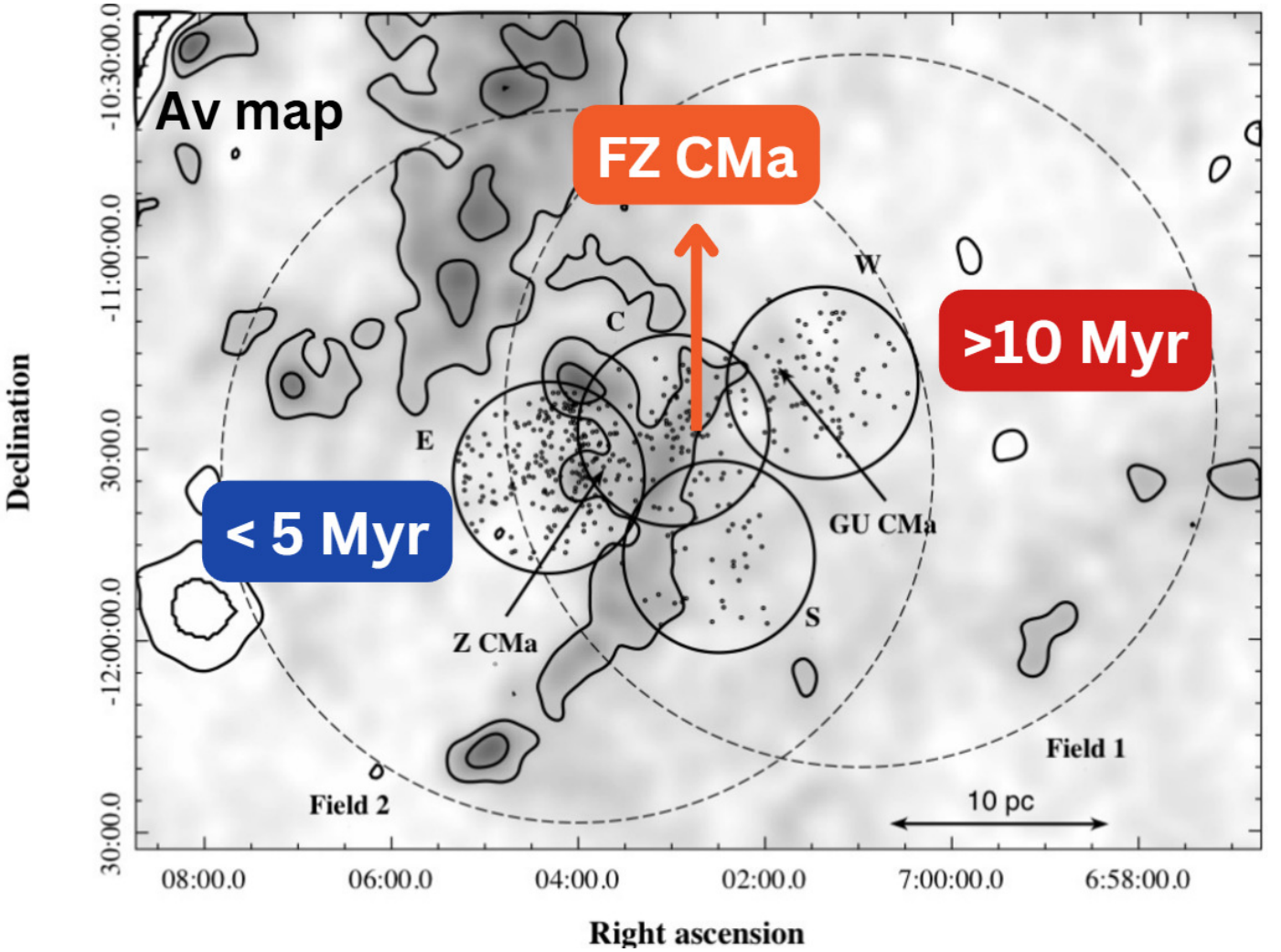


**FIGURE 1.** XMM-Newton fields studied by Santos-Silva et al. (2018) (small circles, where the X-ray sources are shown by dots), compared with ROSAT fields from Gregorio-Hetem et al. (2009, dashed large circles).  $A_V$  map in the background with  $A_V = 2.0$  and 4.0 mag contours. FZ CMa, GU CMa and Z CMa are indicated by arrows. The mean age found for the populations associated with Z CMa and GU CMa are highlighted in blue and red, respectively. Adapted from Santos-Silva et al. (2018).

sion line and Li I ( $\lambda 6708 \text{ \AA}$ ) absorption line. Figure 2 shows an example of an object exhibiting both features.

Corrêa-Rodrigues & Gregorio-Hetem (2024) initially found 27 TT + 5 candidates. As a follow-up to this work, we flux-calibrated all spectra using the spectrophotometry of a standard star and re-evaluated them. This process led to the identification of four additional candidates. Our findings include 24 stars showing  $H\alpha$  emission and Li I absorption (type 1, for simplicity); 5 stars with Li I and  $H\alpha$  absorption (type 2); and 7 with only  $H\alpha$  emission and no Li (type 3). Altogether, we identified 36 young low-mass stars or PMS candidates, 20 of which are X-ray sources. It is important to note that these numbers represent lower limits due to the presence of too faint stars, leading to underexposed spectra that were not useful.

Objects of types 1 and 2 represent the T Tauri stars in our sample. In particular, objects type 2 are WTT, while objects type 1 could be either WTT or CTT. Further analysis will confirm their classification using the criteria proposed by Barrado y Navascués & Martín (2003) and White & Basri (2003). These criteria compare  $W_{H\alpha}$  to spectral type. Type 3 objects could also be young, however with intermediate mass, or could be main sequence stars with  $H\alpha$  emission (for instance Martín et al. 1998).

### 3. S-PLUS photometry

Gregorio-Hetem et al. (2021, hereafter GH21) analysed multi-band photometric data covering a  $1.4^\circ \times 1.4^\circ$  region of CMa. The data were obtained using the 0.8 m T80-South telescope, encompassing 694 stars and overlapping all four GMOS fields.

In parallel with the spectroscopic analysis, we conducted a photometric study of the CMa region by comparing GH21 photometry with the latest data release from the S-PLUS (internal Data Release 5 — iDR5<sup>1</sup>). This comparison aimed to validate the adopted calibration and identify any differences among them. Our primary goal is to characterize cloud members across several spectral domains.

We analysed photometric data for a subsample of GH21 containing 544 members: 149 previously known and 395 new members (with membership probability  $P > 50\%$ ). We compared theoretical curves from PARSEC (PAдова tRieste Stellar Evolutionary Code<sup>2</sup>), and from MIST (MESA Isochrones & Stellar Tracks Choi et al. 2016; Dotter 2016) with the magnitudes and colours in iDR5 for our sample, following the methodology of GH21. The theoretical models represent 100 Myr —

<sup>1</sup> internal Data Release is available only for collaboration members

<sup>2</sup> v1.2S+ COLIBRI S\_37 version of PARSEC models

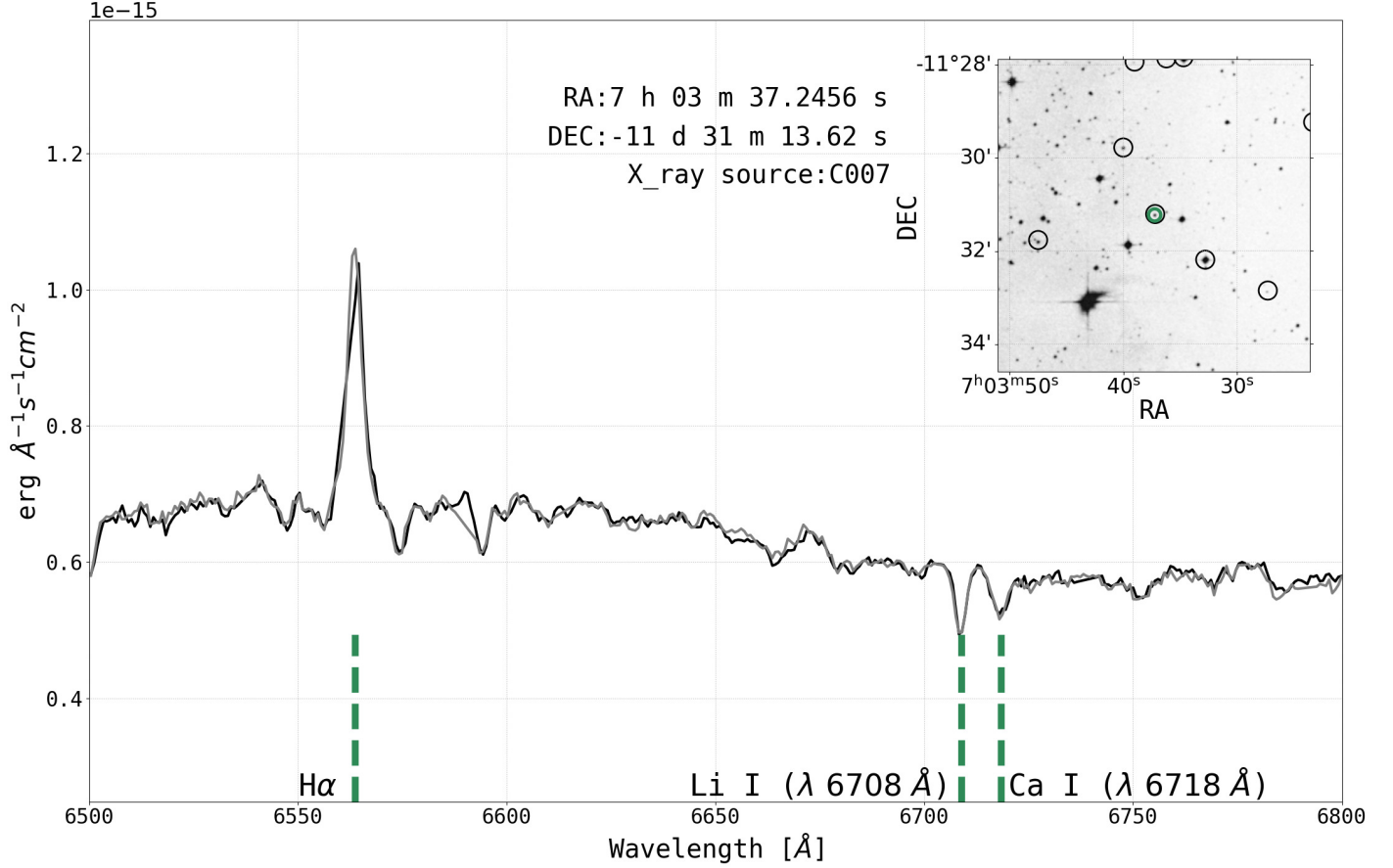


**FIGURE 2.** Examples of two flux-calibrated GMOS spectra of the same star (black and grey lines) showing H $\alpha$  emission and Li I absorption. Ca I ( $\lambda 6718 \text{ \AA}$ ) line is also highlighted to confirm the identification of Li I line. On the top right corner we also indicate the angular position of this object (green circle) compared to the position of X-ray sources (black circles). This example is also an X-ray counterpart.

which is the value adopted to indicate the Zero Age Main-Sequence (ZAMS) — and 5 Myr populations. Two sets of bolometric corrections were used in PARSEC models: YBC + new Vega (YBC for simplicity) and OBC<sup>3</sup>. To complement our iDR5 dataset, we also used estimated photometry from Gaia low-resolution spectra. They were calculated using GaiaXPy (Gaia Collaboration et al. 2023).

Figure 3 shows a colour-colour diagram comparing  $[r' - J0660] \times [r' - i']$  (left panel). Stars with H $\alpha$  excess exhibit  $[r' - J0660]$  indices higher than expected by the theoretical models. These objects were highlighted in green, making a total of 25 stars. The central panel shows  $[u' - g'] \times [g' - r']$ . UV excess is indicated by lower colour indices than the theoretical models. This diagram reveals that all stars with H $\alpha$  excess in our sample and data available in  $u'$ ,  $g'$ , and  $r'$  bands also present UV excess. We also observe a trend that other CMa members present an offset of few tenths of magnitudes when compared to the models. This is also observed in Venuti et al. (2014). These authors suggest that this offset may be related to a population with lower than solar metallicities. However, further analysis is necessary to confirm this hypothesis.

The right panel shows a colour-magnitude diagram. We estimate a mean age of 5 Myr for our sample, though an apparent age dispersion can be seen. Additionally, there is a noticeable lack of high-mass stars in the iDR5 sample, which is compensated by estimated photometry from Gaia, as indicated by blue

points. This is possibly a result from saturation effects affecting the brightest stars.

Compared to GH21, we identified a similar number of stars with H $\alpha$  excess and a similar mean age of 5 Myr for our sample. However, our analysis revealed lower dispersion and more reliable indications of UV excess. Both H $\alpha$  excess and UV excess are probably linked to accretion activity.

#### 4. Conclusion

This study combined spectroscopy and photometric data to investigate the CMa star-forming region. From the GMOS spectra, we identified 36 objects (29 TT + 7 PMS candidates) in the region associated with FZ CMa based on H $\alpha$  emission and Li I ( $\lambda 6708 \text{ \AA}$ ) absorption.

Our multi-band photometric data indicate the presence of stars with H $\alpha$  and UV excess probably related to accretion activity. A mean age of 5 Myr was also estimated for our sample.

The next steps in this work include classifying the objects identified with GMOS spectroscopy as either CTT or WTT. Additional photometric surveys, such as Gaia, Two Micron All Sky Survey (2MASS, Skrutskie et al. 2006), and Wide-field Infrared Survey Explorer (WISE, Wright et al. 2010), will provide information about the membership and the presence of circumstellar discs. A crossmatch with S-PLUS data is also necessary to confirm the expected tendencies of accretion activity.

We also intend to extend this analysis to other young stars in the CMa region, determining whether similar tendencies are

<sup>3</sup> see <http://stev.oapd.inaf.it/cgi-bin/cmd> for details

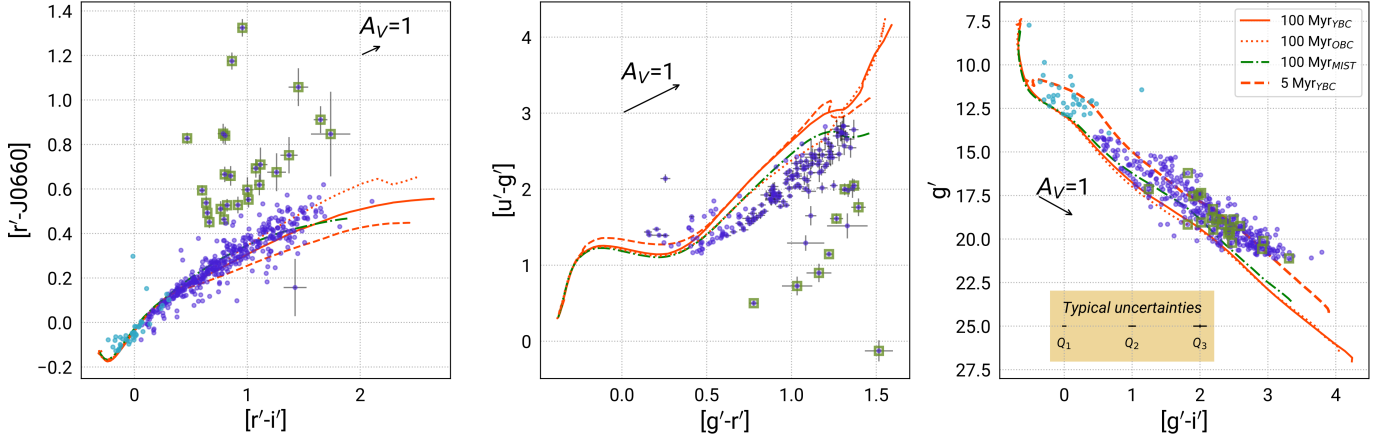


**FIGURE 3.** Comparison between multiband photometric data and theoretical models. Purple points are iDR5 data and blue points are photometric estimates obtained using Gaia low-resolution spectra for stars that were not found in iDR5. Left panel shows 25 stars with  $[r' - J0660]$  excess. These stars are highlighted in all three panels.  $Q_1$ ,  $Q_2$ , and  $Q_3$  in right panel represent first, second, and third quartiles of the uncertainty distribution, respectively.

observed across different areas of the Association. The S-PLUS Ultra-Short Survey will be particularly valuable for complementing our datasets, especially regarding the more massive members of the region.

*Acknowledgements.* We thank the São Paulo Research Foundation (FAPESP) for the financial support (grants #2022/09374-0, #2023/08726-2). We also thank the entire S-PLUS team for their support with S-PLUS data.

## References

- Barrado y Navascués D., Martín E. L., 2003, *AJ*, 126, 2997. doi:10.1086/379673
- Choi J., Dotter A., Conroy C., Cantiello M., Paxton B., Johnson B. D., 2016, *ApJ*, 823, 102. doi:10.3847/0004-637X/823/2/102
- Corrêa-Rodrigues J. V., Gregorio-Hetem J., 2024, *BASBr*, 35, 121
- Dotter A., 2016, *ApJS*, 222, 8. doi:10.3847/0067-0049/222/1/8
- Feigelson E. D., Montmerle T., 1999, *ARA&A*, 37, 363. doi:10.1146/annurev.astro.37.1.363
- Fernandes B., Gregorio-Hetem J., Montmerle T., Rojas G., 2015, *MNRAS*, 448, 119. doi:10.1093/mnras/stv001
- Fernandes B., Montmerle T., Santos-Silva T., Gregorio-Hetem J., 2019, *A&A*, 628, A44. doi:10.1051/0004-6361/201935484
- Gaia Collaboration, Montegriffo P., Bellazzini M., De Angeli F., Andrae R., Barstow M. A., Bossini D., et al., 2023, *A&A*, 674, A33. doi:10.1051/0004-6361/202243709
- Gregorio-Hetem J., Montmerle T., Rodrigues C. V., Marciotto E., Preibisch T., Zinnecker H., 2009, *A&A*, 506, 711. doi:10.1051/0004-6361/200912140
- Gregorio-Hetem J., Navarete F., Hetem A., Santos-Silva T., Galli P. A. B., Fernandes B., Montmerle T., et al., 2021, *AJ*, 161, 133. doi:10.3847/1538-3881/abd705
- Martin E. L., Montmerle T., Gregorio-Hetem J., Casanova S., 1998, *MNRAS*, 300, 733. doi:10.1046/j.1365-8711.1998.01932.x
- Santos-Silva T., Gregorio-Hetem J., Montmerle T., Fernandes B., Stelzer B., 2018, *A&A*, 609, A127. doi:10.1051/0004-6361/201730815
- Skrutskie M. F., Cutri R. M., Stiening R., Weinberg M. D., Schneider S., Carpenter J. M., Beichman C., et al., 2006, *AJ*, 131, 1163. doi:10.1086/498708
- Venuti L., Bouvier J., Flaccomio E., Alencar S. H. P., Irwin J., Stauffer J. R., Cody A. M., et al., 2014, *A&A*, 570, A82. doi:10.1051/0004-6361/201423776
- White R. J., Basri G., 2003, *ApJ*, 582, 1109. doi:10.1086/344673
- Wright E. L., Eisenhardt P. R. M., Mainzer A. K., Ressler M. E., Cutri R. M., Jarrett T., Kirkpatrick J. D., et al., 2010, *AJ*, 140, 1868. doi:10.1088/0004-6256/140/6/1868